Article

Discovery Medicine 2024; 36(191): 2365–2375
https://doi.org/10.24976/Discov.Med.202436191.218

Protective Role of TAOK1-CDC20 Axis in Atherosclerosis: Modulation of Endothelial Apoptosis and Senescence

Yun Qiu[1], Haiwen Zhou[1], Haiqiang Ding[1], Jianzhou Wu[1], Yu Tao[1,*]

[1]Department of Cardiology, Jiangxi Provincial People's Hospital, The First Affiliated Hospital of Nanchang Medical College, 330006 Nanchang, Jiangxi, China
*Correspondence: taoyuk@126.com (Yu Tao)
Published: 20 December 2024

Background: Atherosclerosis, a chronic inflammatory condition characterized by the accumulation of lipid and fibrous elements in the arterial wall, is a major contributor to cardiovascular disease. This study aimed to investigate the regulation of apoptosis and cellular aging in human umbilical vein endothelial cells by Thousand and One Amino Acid Kinase 1 (TAOK1) via Cell division cycle 20 (*CDC20*) in the context of atherosclerosis.

Methods: The study evaluated the impact of TAOK1 on Oxidized low-density lipoprotein (ox-LDL)-induced changes in cell viability, angiogenesis, cell senescence, apoptosis, cell cycle arrest, and related signaling pathways in human umbilical vein endothelial cells (HUVECs) using Cell Counting Kit-8, β-galactosidase staining, flow cytometry, and western blot. The role of *CDC20* as a potential downstream target of TAOK1 was further investigated using specific small interfering (si) RNAs.

Results: Overexpression of TAOK1 partially reversed the ox-LDL-mediated reduction in cell viability and counteracted the increase in pro-inflammatory cytokines and chemokines in HUVECs, with significant differences observed ($p < 0.05$). Ox-LDL-induced decrease in angiogenesis and increase in cell senescence, apoptosis were observed, and cell cycle arrest was alleviated by TAOK1, with all changes being statistically significant ($p < 0.05$). In addition, TAOK1 transfection partially neutralized ox-LDL-induced changes in key downstream pathway proteins, including CDC20, phosphorylated p65 (p-p65), β-catenin, and glycogen synthase kinase 3 beta (GSK-3β). Co-immunoprecipitation (Co-IP) confirmed the regulatory interaction between TAOK1 and CDC20. The inhibitory effects of TAOK1 on ox-LDL-induced cellular changes were significantly reversed by *CDC20* siRNA ($p < 0.05$), highlighting the role of CDC20 in the protective mechanisms mediated by TAOK1.

Conclusions: TAOK1 plays a pivotal role in protecting endothelial cells from ox-LDL-induced cellular stress in the atherosclerotic environment, primarily by modulating pro-inflammatory responses, angiogenesis, cell senescence, and apoptosis. This study provides important insights into the protective mechanisms of TAOK1 and its interplay with downstream signaling molecules, particularly CDC20, in the vascular endothelium under atherosclerotic conditions.

Keywords: TAOK1; CDC20; atherosclerosis; HUVECs; Wnt/β-catenin; NF-κB

Introduction

Atherosclerosis, a complex disease marked by the accumulation of plaque in the artery wall, is a major cause of death globally [1]. The process involves an intricate interaction between the buildup of lipids, persistent inflammation, impaired functioning of the endothelium, and the restructuring of blood vessels [2]. The endothelium has a crucial function in preserving vascular homeostasis [3]. Atherosclerosis can cause venous endothelial damage, which can indirectly exacerbate the onset and progression of atherosclerosis through thrombosis, inflammatory response, and vascular remodeling [4,5]. Understanding these mechanisms can help reveal the interrelationship between venous and arterial diseases and provide new ideas for the prevention and treatment of related diseases. Human umbilical vein endothelial cells (HUVECs), have been thoroughly investigated to explore the pathophysiology of atherosclerosis, which is because these cells play a crucial role in regulating vascular tone, permeability, and hemostasis [6,7]. Despite progress in understanding and treating this pervasive disease, current therapeutic strategies primarily focus on symptom management rather than altering disease progression. Therefore, comprehending the pathomechanisms of atherosclerosis will aid in identifying new therapeutic targets, providing a theoretical foundation for the development of clinical drugs aimed at atherosclerosis.

Atherosclerosis begins with endothelial damage, which triggers a series of inflammatory reactions and the buildup of lipids in the artery wall [8]. Oxidized low-density lipoprotein (ox-LDL) contributes to plaque formation by promoting foam cell formation and triggering en-

dothelial cell dysfunction [9]. Atherosclerosis is marked by a decrease in the availability of nitric oxide (NO), an increase in the permeability of the endothelium, and the activation of adhesion molecules and chemokines, which results in the recruitment of more inflammatory cells [10]; this, in turn, induces a series of oxidative stress responses, including reactive oxygen species (ROS) accumulation, apoptosis, and cellular senescence [11]. Excessive apoptosis of endothelial cells plays a role in the development of atherosclerosis by increasing the instability of plaques [12]. However, cell senescence, during which cells permanently stop dividing, promotes atherosclerosis by releasing substances that cause inflammation and contribute to the development of plaque in the arteries; this process characterizes the senescence-associated secretory phenotype [13].

Gaining insight into the molecular pathways that cause endothelial cell failure, apoptosis, and senescence in atherosclerosis is essential for the development of specific treatments. Thousand and One Amino Acid Kinase 1 (TAOK1), a member of the mitogen-activated protein (MAP) kinase family, has a role in reducing inflammation in many types of cells, and this process involves several pathways, including nuclear factor kappa-B (NF-κB) and Wingless/Integrated (Wnt)/β-catenin [14,15]. Nevertheless, the involvement of TAOK1 in inflammation resulting from endothelial cell damage remains uncertain. Cell division cycle 20 (CDC20) is an activator of the anaphase-promoting complex/cyclosome, which is involved in several biological activities, such as controlling the cell cycle and promoting programmed cell death [16]. Several diseases, including atherosclerosis, have been linked to the dysregulation of CDC20 in the cardiovascular system [17]. Currently, there is a lack of studies focused on the binding between TAOK1 and CDC20, as well as the potential consequences of their interactions.

Clarifying the interaction between TAOK1 and CDC20, and their effects on subsequent pathways, including NF-κB and Wnt/β-catenin, is critical for understanding their complex functions in endothelial cell biology. The activation of NF-κB, a well-recognized transcription factor implicated in inflammatory reactions, occurs in endothelial cells as a result of several stress stimuli, such as ox-LDL [18]. The Wnt/β-catenin pathway is critical for controlling cell proliferation, differentiation, and survival [19]. The connection between TAOK1 and CDC20 modulates these pathways, offering a fresh insight into the molecular processes that regulate endothelial cell responses in atherosclerosis.

Understanding the intricate mechanisms by which TAOK1 and CDC20 affect the activity of endothelial cells is crucial due to the intricate nature of atherosclerosis and the significant role played by endothelial cells in its progression. An improved understanding presents the possibility of innovative treatment approaches that focus on addressing endothelial cell dysfunction, apoptosis, and senescence in atherosclerosis. The objective of this research is to clarify the function of TAOK1 in regulating the reactions of HUVECs, specifically via its connection with CDC20. Furthermore, it aims to uncover how this interaction modulates key signaling pathways that contribute to the endothelial injury mechanisms underlying atherosclerosis.

Table 1. The sequence of *CDC20* small interfering (si) RNAs and si-NC.

Gene	Sequence 5′-3′
CDC20 siRNA-1 sense	GCACAGAACCAGCUAGUUAUU
CDC20 siRNA-1 antisense	UAACUAGCUGGUUCUGUGCAA
CDC20 siRNA-2 sense	CCACCAUGAUGUUCGGGUAGC
CDC20 siRNA-2 antisense	UACCCGAACAUCAUGGUGGUG
si-NC sense	AAUCUGACACUUAUCCGAGAG
si-NC antisense	AUGGUCUGACUGACAUUGUCA

CDC20, Cell division cycle 20; si-NC, si-negative control.

Materials and Methods

Cell Culture

HUVECs from ATCC (CRL-1730, Rockefeller, MD, USA) were identified by Short Tandem Repeats (STR) and tested for mycoplasma, and cultured in endothelial cell culture medium (CM-0122, ProCell, Wuhan, China) supplemented with 10% fetal bovine serum (10091148, Gibco, Thermo Fisher Scientific, Waltham, MA, USA). The cells were maintained at 37 °C with 5% CO_2. For experimental procedures, cells between passages 3 and 8 were utilized. To establish the ox-LDL model, HUVECs were exposed to ox-LDL (100 µg/mL; IO1300, Solarbio, Beijing, China) for 24 h at 37 °C to simulate an atherosclerotic environment *in vitro*.

Transfection

The TAOK1 overexpression vector (pcDNA3.1-TAOK1), *CDC20* small interfering (si) RNA (cat no. D-003225-10-0005), and si-negative control (NC) (cat no. D-001210-0X) were purchased from Dharmacon (Lafayette, CO, USA). The sequences of the two siRNAs against *CDC20* as well as the si-NC are shown in Table 1. Transfection was performed using Lipofectamine™ 3000 (L3000015, Invitrogen, Thermo Fisher Scientific) according to the manufacturer's instructions. Briefly, HUVECs were seeded in 6-well plates and grown to 70%–80% confluence. For transfection, the cells were incubated with the transfection mixture containing the vector or siRNA and Lipofectamine™ 3000 reagent for 4 hours, followed by replacement with fresh medium. Transfection efficiency was measured by reverse transcription-quantitative polymerase chain reaction (RT-qPCR).

Angiogenesis Assay

To explore the angiogenic capabilities of HUVECs, we employed the Matrigel tube formation technique. Pre-chilled Matrigel (356237, Corning Inc., Corning, NY, USA) was plated in 50 µL volumes per well in a 96-well format and polymerized at 37 °C for half an hour. HUVECs, at a concentration of 20,000 cells per well, were cultivated on this prepared substrate and maintained at 37 °C. Tube formation was assessed after 4 hours via light microscopy (CKX53, Olympus, Tokyo, Japan), with the extent of tube structures quantified using ImageJ (version 1.8.0; National Institutes of Health, Bethesda, MD, USA).

Cellular Senescence Assay

The assessment of cellular aging involved the use of a beta-galactosidase staining protocol tailored for senescent cells. Cells underwent fixation in 4% paraformaldehyde for 15 minutes at 21 °C, followed by overnight staining with SA-β-gal solution from Beyotime (C0602, Shanghai, China), at 37 °C in a non-CO_2 environment. After staining, cells were rinsed and the senescent (blue-stained) versus non-senescent cells were counted under a light microscope (CKX31, Olympus).

Flow Cytometry

Apoptosis and cell cycle analysis were conducted using flow cytometry. For apoptosis, HUVECs were stained with Annexin V-FITC and propidium iodide (PI) using an Apoptosis Detection Kit (556547, BD Biosciences, Franklin Lake, NJ, USA). For cell cycle analysis, cells were fixed in 70% ethanol, treated with RNase A, and stained with PI. Data acquisition was performed on a BD LSR-Fortessa cell analyzer (BD Biosciences), and data were analyzed using FlowJo™ software (version 10; BD Biosciences).

Detection of ROS

To evaluate the oxidative stress induced by ox-LDL in HUVECs and the effect of TAOK1 overexpression or/and *CDC20* siRNA, we performed ROS detection using the 2′,7′-dichlorofluorescein diacetate (DCFDA) Cellular ROS Detection Assay Kit (S0033S, Beyotime, Shanghai, China). HUVECs were treated with DCFDA reagent under standard conditions, followed by incubation to facilitate reaction with ROS, forming the fluorescent dichlorofluorescein (DCF). The fluorescence was then quantified to assess ROS levels using a microplate reader (multiscan MK3, Thermo Fisher Scientific).

RT-qPCR

Total RNA was extracted from HUVECs using the RNeasy Mini Kit (74104, Qiagen, Hilden, Germany). cDNA was synthesized using 2×NovoScript® Plus 1st Strand cDNA Synthesis SuperMix (E047-01A, Novoprotein, Suzhou, China). qRT-PCR reactions were performed using NovoStart® SYBR qPCR SuperMix Plus (E096-01A, Novoprotein). PCR conditions were as follows: 95 °C for 1 min, followed by 40 cycles of 95 °C for 20 s, 56 °C for 20 s, and extension for 38 s. Data analysis was performed using the $2^{-\Delta\Delta CT}$ method. Primer sequences for *TAOK1*, *CDC20*, monocyte chemoattractant protein-1 (*MCP-1*), vascular cell adhesion molecule-1 (*VCAM-1*), intercellular adhesion molecule-1 (*ICAM-1*), and the housekeeping gene Glyceraldehyde-3-phosphate dehydrogenase (*GAPDH*) (all from Ribobio, Guangzhou, China) are listed in Table 2.

Table 2. Primer sequences used in RT-qPCR.

Gene	Sequence 5′-3′
TAOK1-F	CTGCCATGGAGAAAGAGGCTAA
TAOK1-R	TCTTCTTCTGCTTGGAAATGCTG
CDC20-F	CAGTGCTGAGGTGCAGCTAT
CDC20-R	ACATGGTGTTCTGCTACCCG
MCP-1-F	TCAAACTGAAGCTCGCACTCT
MCP-1-R	GCATTGATTGCATCTGGCTG
VCAM-1-F	GGATAATGTTTGCAGCTTCTCAAG
VCAM-1-R	ATTCGTCACCTTCCCATTCAGT
ICAM-1-F	GGAGCTTCGTGTCCTGTATGG
ICAM-1-R	CAGTGGGAAAGTGCCATCCT
GAPDH-F	GCTCATTTGCAGGGGGGAG
GAPDH-R	GTTGGTGGTGCAGGAGGCA

RT-qPCR, reverse transcription-quantitative polymerase chain reaction; *TAOK1*, Thousand and One Amino Acid Kinase 1; *MCP-1*, monocyte chemoattractant protein-1; *VCAM-1*, vascular cell adhesion molecule-1; *ICAM-1*, intercellular adhesion molecule-1; *GAPDH*, Glyceraldehyde-3-phosphate dehydrogenase.

Western Blot

To assess protein expression in HUVECs, the cells were first disrupted using a lysis buffer from Solarbio (R0010, Beijing, China), and protein concentrations were quantified using a bicinchoninic acid (BCA) assay kit from Solarbio (PC0020), as per the provided guidelines. Proteins (20 µg per sample) were then resolved on a 10% sodium dodecyl sulfate-polyacrylamide gel electrophoresis and subsequently electrotransferred onto polyvinylidene difluoride membranes supplied by MilliporeSigma (03010040001, Burlington, MA, USA). Following the transfer, membranes were blocked for one hour at 21 °C using skim milk (D8340, Solarbio). Incubation with primary antibodies was performed overnight at 4 °C, using antibodies (Abcam, Cambridge, UK) against TAOK1 (1:1000; ab197891), CDC20 (1:2000; ab183479), phosphorylated (p)-p65 (1:1000; ab76302), p65 (1:1000; ab32536), glycogen synthase kinase 3 beta (GSK-3β) (1:2000; ab32391), β-catenin (1:1000; ab305261), and GAPDH (1:3000; ab181602). Then, membranes were

treated with a secondary Goat anti-rabbit Immunoglobulin G (IgG) (ab205718, Abcam) at a dilution of 1:2000 for two hours. Protein bands were visualized using the Enhanced Chemiluminescence system from Thermo Fisher Scientific. The relative abundance of protein bands was quantitatively analyzed with ImageJ software, and protein expression levels were normalized to GAPDH as a loading control.

Cell Counting Kit-8 Assay

A Cell Counting Kit-8 (CCK-8) (C0038, Beyotime, Shanghai, China) was used to determine the viability of the cells. In 96-well plates, HUVECs were seeded and given care in accordance with the experimental setup. CCK-8 solution was added 24 hours after ox-LDL treatment or RNA transfection, and the plates were then incubated for 2 hours at 37 °C. Optical density (OD) was measured at 450 nm using a microplate reader (multiscan MK3, Thermo Fisher Scientific). The calculation formula is as follows:

$$\textit{Cell viability (\%)} = [(OD_E - OD_B)/(OD_C - OD_B)] \times 100\%$$

OD_E, OD value of the experimental group; OD_C, OD value of the control group; OD_B, OD value of the blank group.

Enzyme-Linked Immunosorbent Assay (ELISA)

Following the manufacturer's instructions, ELISA kits from Solarbio (Beijing, China) were used to quantify the amounts of interleukin (IL)-1β (SEKH-0002), IL-6 (SEKH-0013), and IL-8 (SEKH-0016) in the culture supernatants of HUVECs. Using a microplate reader, OD—which is correlated with the amount of cytokines in the samples—was determined at 450 nm. By comparing the absorbance readings to the standard curve, it was possible to calculate the concentration of each cytokine in the samples.

NO Detection

NO concentration in the culture supernatant of HUVECs was quantified using the Micro NO Content Assay Kit (BC1475, Solarbio) following the manufacturer's instructions. NO is highly susceptible to oxidation, forming NO^{2-}, which reacts with diazotized sulfanilamide to produce a diazo compound. This compound subsequently couples with N-(1-naphthyl)ethylenediamine to form a chromophoric product with a characteristic absorption peak at 550 nm. The absorbance at 550 nm was measured using a microplate reader. By comparing the absorbance values with a standard curve, the NO concentration in the samples was calculated.

Co-Immunoprecipitation (Co-IP)

Co-IP was used to examine how the TAOK1 and CDC20 proteins interacted. Following a 4-hour transfection of CDC20 siRNA with TAOK1, new media were added, and cells were harvested 48 hours later at 37 °C. Cells were lysed using Beyotime's RIPA lysate. The BCA Kit was used to determine the amount of protein in the lysates. To lessen non-specific binding, the lysates were pre-cleared by being incubated for an hour at 4 °C with Protein G Agarose beads (Roche). Following pre-clearing, the lysates were incubated overnight at 4 °C with gentle rotation with 2 µg of either TAOK1 or CDC20 antibody. After removing any non-specifically bound proteins from the beads using four rounds of lysis buffer washing, a western blot analysis was performed utilizing antibodies against TAOK1 and CDC20.

Data Analysis

GraphPad Prism 8 (Dotmatics, New York, NY, USA) was used for data analysis. The data are shown as the mean $\pm$ standard deviation. For comparisons between the two groups, the unpaired Student's *t*-test was used. When comparing several groups, a one-way or two-way analysis of variance was used, and Tukey's post-hoc test was used for pairwise comparisons. p values < 0.05 were considered statistically significant.

Results

TAOK1 Overexpression and its Effects on HUVECs

Compared to the control (100% $\pm$ 1.48%), ox-LDL induced a reduction in cell viability (60.26 $\pm$ 2.01%; $p < 0.05$) (Fig. 1A), which confirmed the model construction. Ox-LDL also induced a decrease in *TAOK1* expression (Fig. 1B,C). We constructed a *TAOK1* overexpression vector and transfected it into HUVECs. The results of RT-qPCR indicated that the transfection efficiency of the vector was 83.33%. Compared with the NC group (0.99 $\pm$ 0.01), the transfection of the *TAOK1* overexpression vector resulted in an increase in *TAOK1* mRNA levels (6.34 $\pm$ 0.38; $p < 0.05$) (Fig. 1D). Western blot analysis showed that relative to the NC group (1.06 $\pm$ 0.05), transfection with the *TAOK1* overexpression vector significantly enhanced the TAOK1 protein level (1.65 $\pm$ 0.11; $p < 0.05$) (Fig. 1E). Next, we transfected *TAOK1* into HUVECs treated with ox-LDL and observed that the reduction in cell viability mediated by ox-LDL was partly reversed by TAOK1 (Fig. 1F); there was no significant difference between the NC and control groups. Additionally, TAOK1 counteracted the ox-LDL-mediated increase in pro-inflammatory cytokines IL-1β, IL-6, and IL-8 (Fig. 1G), and in the ROS level (Fig. 1H). Consistent with role of pro-inflammatory cytokines as chemokines, *TAOK1* partially counteracted the ox-LDL-mediated increase in gene expression of *MCP-1*, *VCAM-1*, and *ICAM-1* (Fig. 1I). In addition, whereas ox-LDL promoted NO release (99.71 $\pm$ 0.87%; $p < 0.05$) compared to the NC group (31.33 $\pm$ 2.08%), TAOK1 partially blocked the effect of ox-LDL (61.13 $\pm$ 8.01%) (Fig. 1J); there was no significant difference between the NC and control groups. These findings highlight the efficacy of TAOK1 overexpression in mitigating ox-LDL-induced cellular stress.

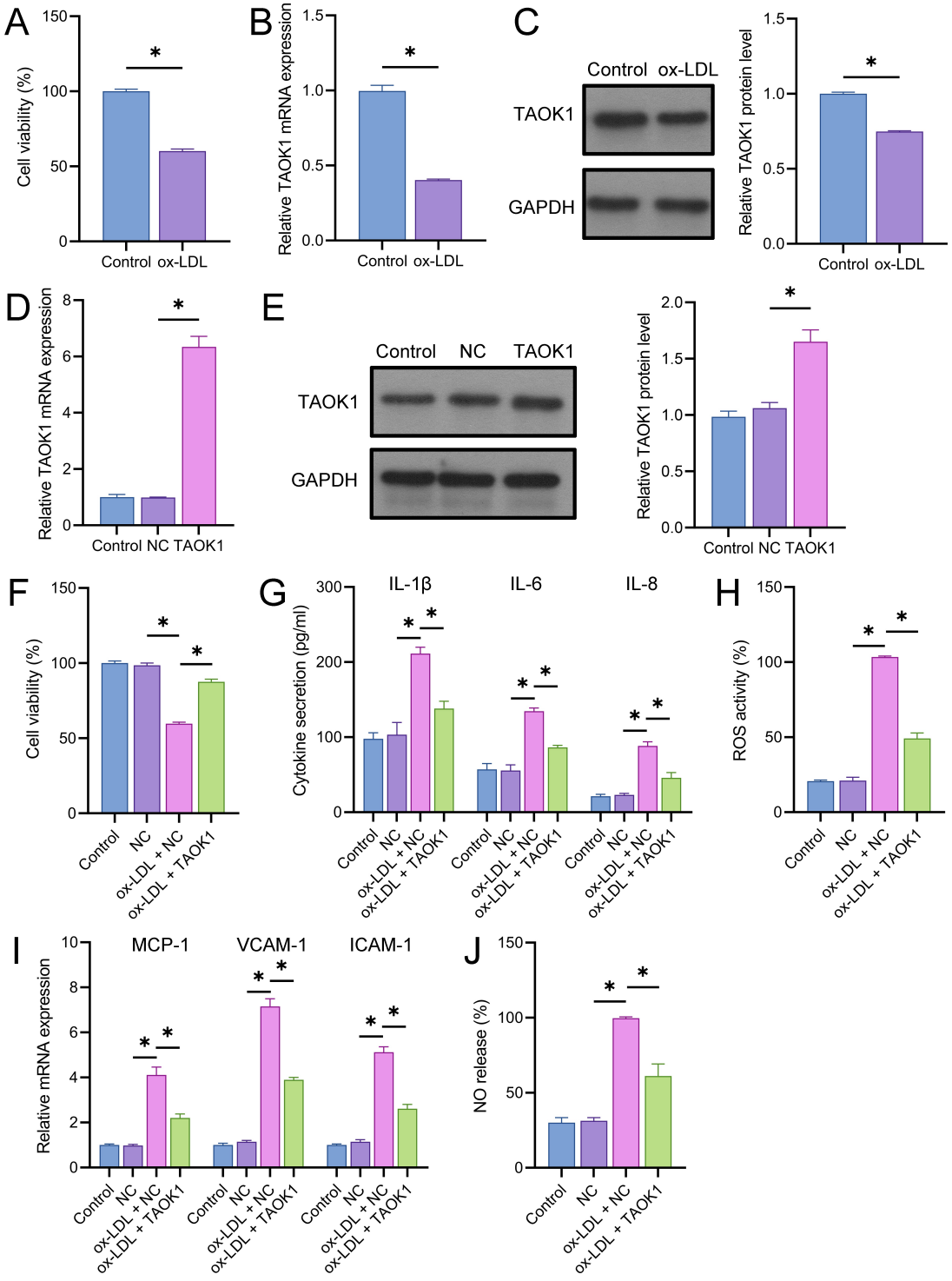

Fig. 1. TAOK1 overexpression and its effect on human umbilical vein endothelial cells (HUVECs) under Oxidized low-density lipoprotein (ox-LDL) stress. (A) Cell Counting Kit-8 (CCK-8) was used to assess cell viability (n = 3). (B) RT-qPCR was used to assess *TAOK1* expression (n = 3). (C) Western blot was used to assess TAOK1 protein level (n = 3). (D) RT-qPCR was used to verify the validity of the *TAOK1* vector (n = 3). (E) Western blot was used to verify the validity of the TAOK1 vector (n = 3). (F) CCK-8 was used to evaluate the effect of TAOK1 on cell viability (n = 3). (G) Enzyme-linked immunosorbent assay (ELISA) was used to evaluate the effect of TAOK1 on interleukin (IL)-1β, IL-6, and IL-8 (n = 3). (H) Detection of reactive oxygen species (ROS) production (n = 3). (I) RT-qPCR analysis shows the effect of *TAOK1* in partially counteracting the ox-LDL-mediated increase in chemokine gene expression (*MCP-1*, *VCAM-1*, *ICAM-1*) (n = 3). (J) Measurement of nitric oxide (NO) release showing that TAOK1 partially blocked the inhibitory effect of ox-LDL (n = 3). *$p < 0.05$.

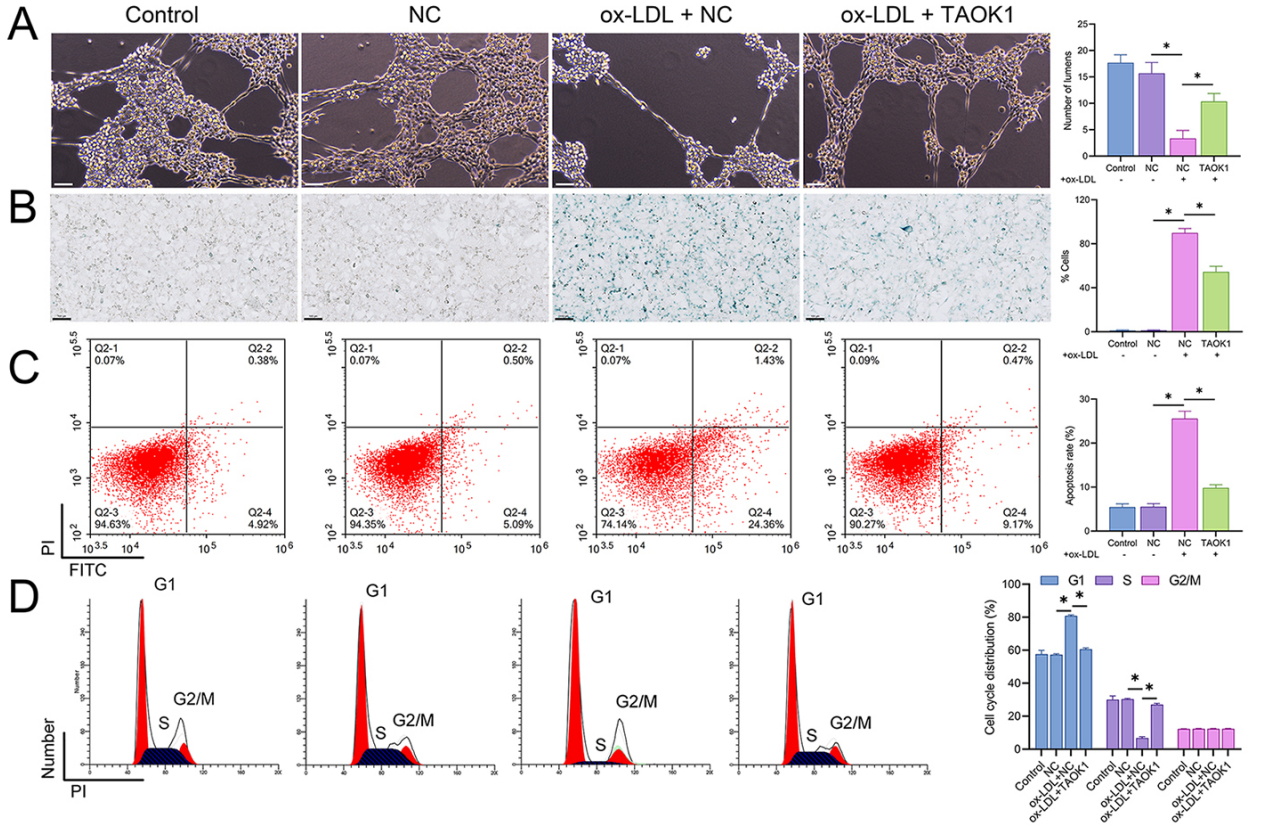

Fig. 2. Mitigating effects of TAOK1 on vascular damage induced by ox-LDL. (A) Angiogenesis assay of the effect of TAOK1 transfection on HUVECs (Scale = 50 µm) (n = 3). (B) β-Galactosidase was used to assess the effect of TAOK1 transfection on cell senescence in HUVECs (Scale = 100 µm) (n = 3). (C,D) Flow cytometry was used to assess the effect of TAOK1 transfection on apoptosis (n = 3) and the cell cycle (G1, S, G2/M) (n = 3). *$p < 0.05$.

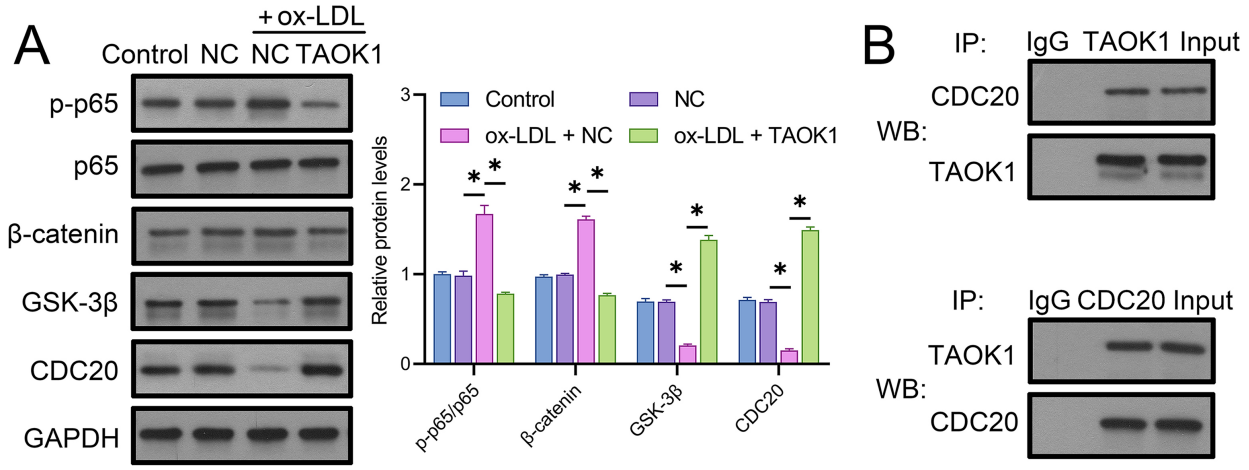

Fig. 3. TAOK1 effects on downstream signaling and interaction with CDC20. (A) Western blot analysis depicting the modulation of protein levels of phosphorylated p65 (p-p65), p65, β-catenin, GSK-3β, and CDC20 by TAOK1 in ox-LDL-treated HUVECs (n = 3). (B) Co-immunoprecipitation (Co-IP) demonstrates the interaction between TAOK1 and CDC20 (n = 3). *$p < 0.05$. IgG, Immunoglobulin G; GSK-3β, glycogen synthase kinase 3 beta.

TAOK1's Role in Mitigating Vascular Damage

The results revealed that, compared to the NC group, treatment with ox-LDL resulted in a marked decrease in angiogenesis ($p < 0.05$) (Fig. 2A). The number of senescent cells was higher after ox-LDL treatment compared with the NC group ($p < 0.05$), indicating accelerated cellular senescence (Fig. 2B). Apoptosis rates, assessed by flow cytom-

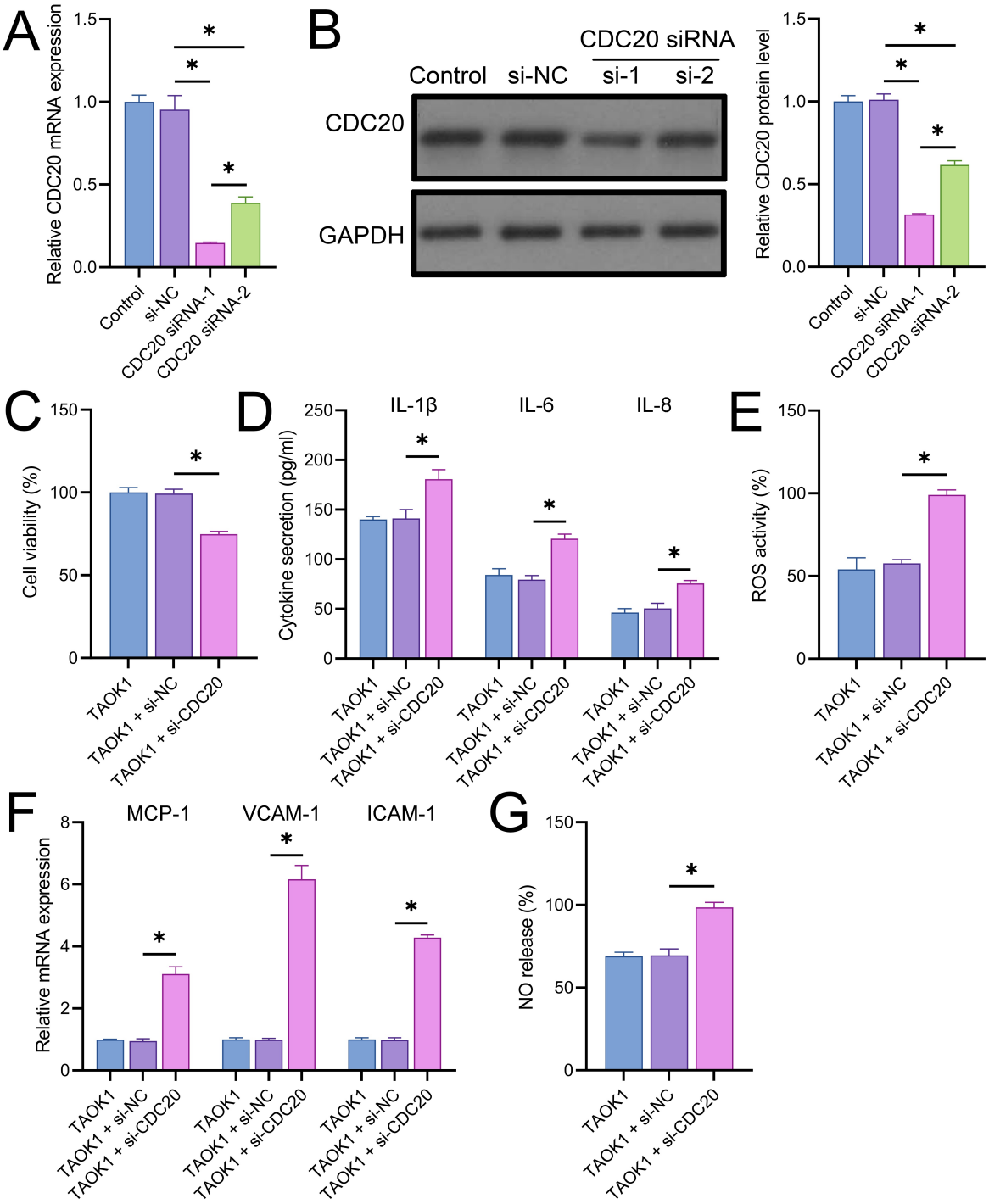

Fig. 4. Effect of CDC20 siRNA on TAOK1-mediated protective mechanisms in HUVECs. (A) RT-qPCR was used to assess the efficiency of CDC20 siRNA (n = 3). (B) Western blot was used to assess the efficiency of CDC20 siRNA (n = 3). (C) CCK-8 assay showing the reversal of cell viability improvement by CDC20 siRNA under ox-LDL-induced condition (n = 3). (D) ELISA analysis of the effect of CDC20 siRNA on TAOK1-mediated IL-1β, IL-6, and IL-8 under ox-LDL-induced condition (n = 3). (E) Detection of the effect of CDC20 siRNA on TAOK1-mediated ROS activity under ox-LDL-induced condition (n = 3). (F) RT-qPCR was used to assess CDC20 siRNA on TAOK1-mediated chemokine gene expression (*MCP-1*, *VCAM-1*, *ICAM-1*) under ox-LDL-induced condition (n = 3). (G) Assessment of NO release showing inhibition by CDC20 siRNA under ox-LDL-induced condition (n = 3). *$p < 0.05$.

etry analysis, were significantly elevated in HUVECs exposed to ox-LDL ($p < 0.05$), demonstrating an increase in apoptotic cell death (Fig. 2C); there was no significant difference between the NC and control groups. Furthermore, cell cycle analysis revealed an increase in cell cycle arrest at the G1 phase in the ox-LDL treated cells, as shown by

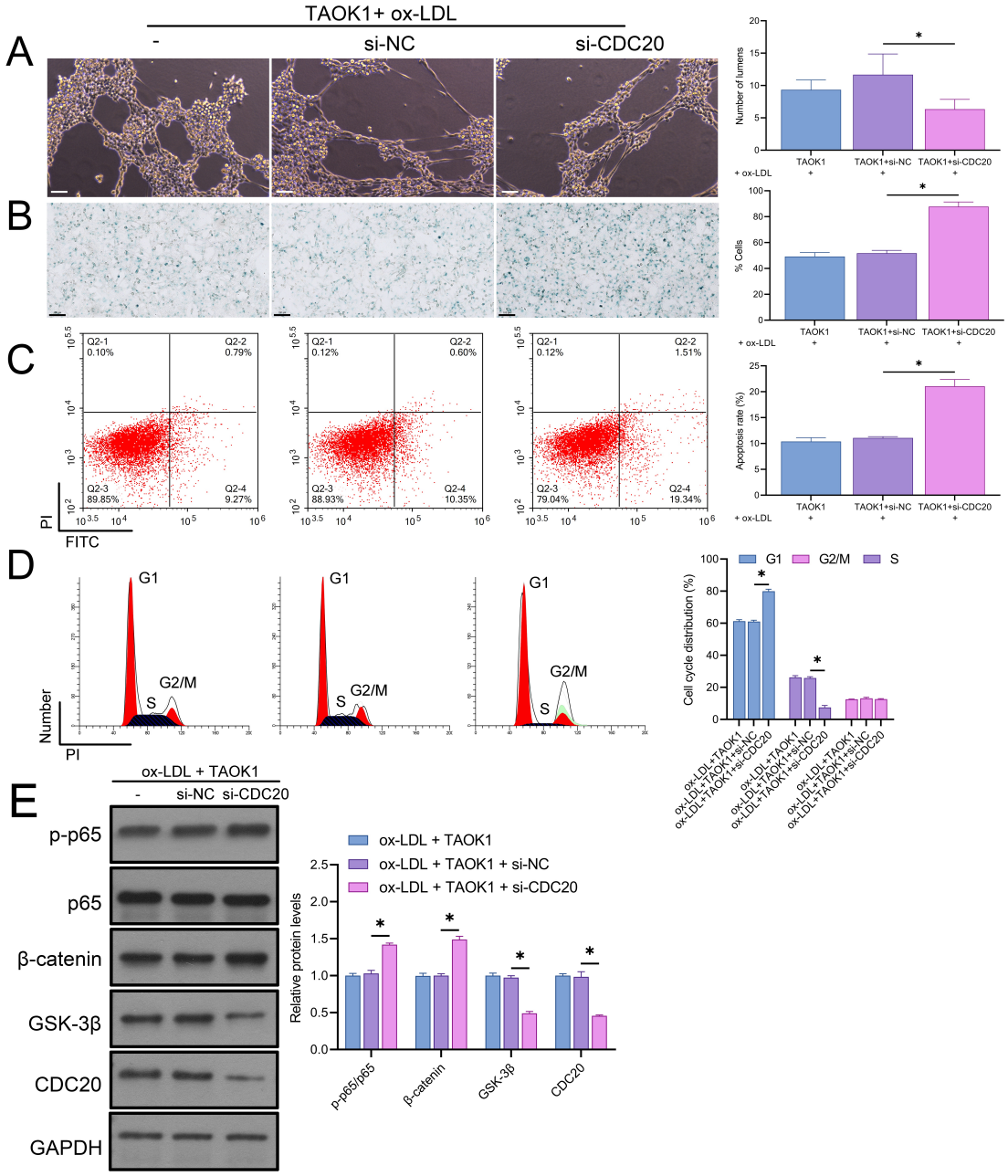

Fig. 5. Impact of CDC20 siRNA on TAOK1-mediated protective mechanisms. (A) Angiogenesis assay analysis of the effect of CDC20 siRNA on TAOK1-mediated angiogenesis (Scale = 50 µm) (n = 3). (B) β-Galactosidase was used to assess CDC20 siRNA on TAOK1-mediated cell senescence (Scale = 100 µm) (n = 3). (C,D) Flow cytometry was used to assess CDC20 siRNA on TAOK1-mediated apoptosis (n = 3) and cell cycle (G1, S, G2/M) (n = 3). (E) Western blot was used to assess CDC20 siRNA on TAOK1-mediated protein levels of p-p65, p65, β-catenin, GSK-3β, and CDC20 (n = 3). *$p < 0.05$.

a higher percentage of cells in this phase compared to the NC group ($p < 0.05$) (Fig. 2D); there was no significant difference between the NC and control groups. All of these ox-LDL-induced changes were significantly attenuated after transfection with TAOK1 ($p < 0.05$). These findings confirm that TAOK1 is a pivotal protein in reducing ox-LDL-induced cellular damage and aging.

Effect of TAOK1 on Downstream Signaling

In order to explore the mechanisms by which TAOK1 delays cellular damage and aging, we analyzed its effects on downstream signaling pathways. The results showed that in HUVECs treated with ox-LDL, protein levels of phosphorylated p65 (p-p65) (1.67 $\pm$ 0.10) and β-catenin (1.61 $\pm$ 0.04) were increased, whereas GSK-3β (0.21 $\pm$ 0.02) and CDC20 (0.15 $\pm$ 0.02) levels were decreased (all $p < 0.05$)

compared to the NC group (0.98 ± 0.05; 1.00 ± 0.01; 0.69 ± 0.02; 0.69 ± 0.03). However, these effects were partially neutralized after TAOK1 transfection (0.78 ± 0.02; 0.77 ± 0.02; 1.38 ± 0.05; 1.49 ± 0.04) (Fig. 3A), suggesting that CDC20 might be a target of TAOK1 and that TAOK1 could inactivate downstream NF-κB and Wnt/β-catenin signaling via CDC20. Subsequently, the interaction between TAOK1 and CDC20 was confirmed by Co-IP (Fig. 3B). This suggests that TAOK1 modulates key signaling pathways, potentially offering a therapeutic target for vascular pathologies.

Effect of CDC20 siRNA on TAOK1-Mediated Protective Mechanisms

We transfected two different siRNAs targeting *CDC20* into HUVECs and assessed their inhibitory efficiency. The results of RT-qPCR indicated that the transfection efficiency of the *CDC20* siRNA was 76.67%. RT-qPCR and western blot results showed that siRNA-1 had significantly higher inhibitory efficiency (85.23%, 68.33%) than siRNA-2 (61.10%, 38.33%), with no significant difference between the si-NC and control groups (Fig. 4A,B). Thus, siRNA-1 was selected as the knockdown vector for CDC20 in subsequent mechanistic analyses. To explore the combined effect of TAOK1 and CDC20 on cellular aging, we co-transfected *TAOK1* and *CDC20* siRNA into HUVECs. CCK-8 results revealed that amelioration of ox-LDL-induced reduction in cell viability by *TAOK1* was reversed by *CDC20* siRNA; there was no significant difference between the NC and control groups (Fig. 4C). Furthermore, the partial counteraction of ox-LDL-induced pro-inflammatory cytokines, ROS, and chemokines by *TAOK1* was also reversed by *CDC20* siRNA (Fig. 4D–F). The inhibitory effect of *TAOK1* on NO release (69.59 ± 3.91%) was also mitigated by *CDC20* siRNA (98.53 ± 2.98%) (Fig. 4G). These results indicate that CDC20 siRNA has the capacity to reverse the anti-inflammatory effects of TAOK1 on HUVECs.

CDC20 siRNA's Role in Counteracting TAOK1's Effects

The results indicate that in the presence of TAOK1, si-NC did not significantly affect the role of TAOK1 in angiogenesis, cell senescence, apoptosis, or the cell cycle. However, after transfection with CDC20 siRNA, there was a significant reduction in angiogenesis ($p < 0.05$) (Fig. 5A), and increases in cell senescence (Fig. 5B), apoptosis levels ($p < 0.05$) (Fig. 5C), and cell cycle arrest (Fig. 5D), with no significant difference between the TAOK1+si-NC and TAOK1 groups. The NF-κB and Wnt/β-catenin signaling pathways, which were inactivated by TAOK1, were reactivated under the influence of CDC20 siRNA (Fig. 5E). These results indicate that CDC20 siRNA has the ability to reverse the anti-apoptotic and anti-aging effects of TAOK1 on HUVECs.

Discussion

The present study elucidates the protective role of TAOK1 in HUVECs under oxidative stress conditions, particularly those induced by ox-LDL. Our results demonstrate that overexpression of TAOK1 plays a critical role in alleviating ox-LDL-induced cellular stress, as evidenced by the reversal of decreased cell viability, reduction of pro-inflammatory cytokines and chemokines, and enhancement of NO release. These observations provide important insights into the molecular dynamics of endothelial cells in the context of vascular pathologies, particularly atherosclerosis.

Ox-LDL is recognized as a key factor in the progression of atherosclerosis, mainly due to its ability to induce endothelial dysfunction, a key event in the early stages of the disease [20]. The oxidative stress environment characteristic of atherosclerotic lesions is effectively mimicked by our ox-LDL model, as indicated by the observed accumulation of ROS. Dysregulated angiogenesis, a consequence of this stress, can lead to plaque instability and rupture [21]. Our results suggest that TAOK1 may be a key gene in balancing angiogenesis in stressed HUVECs, thereby contributing to plaque stability and integrity, modulating TAOK1 expression could offer a novel approach to protect against endothelial dysfunction and thus, atherosclerosis. The acceleration of cell senescence, apoptosis, cell cycle arrest, and ROS levels induced by ox-LDL were all attenuated to some extent after TAOK1 transfection. This highlights the multifaceted role of TAOK1 in maintaining endothelial integrity and functionality under oxidative stress and confirms its anti-apoptotic and anti-senescent properties, consistent with previous research on its protective role in cardiovascular diseases [22]. Inflammation, a hallmark of atherosclerosis, is critically driven by the endothelial response to ox-LDL [23]. Our research demonstrates that the overexpression of TAOK1 can reduce pro-inflammatory cytokines and chemokines in HUVECs treated with ox-LDL, aligning with previous findings by Hashimoto *et al.* [24] on the interplay between inflammation/oxidative stress/apoptosis-induced by ox-LDL. Given the role of chronic inflammation in the development of atherosclerosis and its complications, the anti-inflammatory effect of TAOK1 is particularly noteworthy.

Further elucidating the protective mechanisms of TAOK1, our study highlights its role in modulating key signaling pathways implicated in the regulation of apoptosis and senescence. Specifically, the Wnt/β-catenin and NF-κB signaling pathways are critical mediators of cellular responses to stress, including inflammation, apoptosis, and cellular aging. Changes in CDC20, p-p65, β-catenin, and GSK-3β protein levels were observed in ox-LDL-induced HUVECs, suggesting that these molecules are key components of pathophysiological responses to oxidative stress. Importantly, TAOK1 transfection partially

neutralized these changes, suggesting a regulatory role for key pathways, including NF-κB and Wnt/β-catenin. The regulation of these pathways by TAOK1, particularly its interaction with CDC20, provides a potential therapeutic target for vascular disease. Because NF-κB is a key regulator of inflammation, activation of NF-κB by ox-LDL in endothelial cells is a well-recognized mechanism leading to atherosclerosis [18,25]. Similarly, the modulation of Wnt/β-catenin signaling by TAOK1 could underlie its role in inhibiting senescence and promoting cell survival under oxidative stress conditions [26]. By interfering with these pathways, TAOK1 may inhibit the pro-apoptotic and pro-senescent signaling cascades initiated by ox-LDL, highlighting its potential as a protective modulator in endothelial cells.

The interaction between TAOK1 and CDC20, confirmed by Co-IP, is particularly noteworthy. This interaction suggests the existence of a novel regulatory axis in HUVECs through which TAOK1 positively influences CDC20 expression. Given the role of CDC20 in cell cycle progression and apoptosis [27], its regulation by TAOK1 may be a key determinant of the cellular response to oxidative stress. The role of CDC20 in mediating the effects of TAOK1 was further characterized by experiments using CDC20-specific siRNA. The TAOK1-mediated reversal of cell viability, inflammatory responses and improved NO release by CDC20 siRNA indicates that the protective effects of TAOK1 are at least partially dependent on CDC20, suggesting a complex interaction in which the beneficial effects of TAOK1 on HUVECs under ox-LDL stress are mediated by its effects on CDC20. In addition, CDC20 siRNA is able to counteract the effects of TAOK1 in promoting angiogenesis, inhibiting cellular senescence, apoptosis, cell cycle arrest, and ROS accumulation, further confirming the critical role of CDC20 in these processes. The reactivation of NF-κB and Wnt/β-catenin pathways under the influence of CDC20 siRNA highlights the complexity of these signaling networks in HUVECs and their regulation by TAOK1. This study elucidates the role of TAOK1 in regulating apoptosis and senescence through its interaction with CDC20, an endothelial cell oxidative stress mechanism previously unexplored. Furthermore, our research highlights the potential of targeting CDC20 as part of a strategy to enhance endothelial cell resilience against oxidative stress-induced apoptosis and senescence.

This study has limitations. First, the mechanism of action of TAOK1 in this study was only verified in HUVECs and not analyzed in animals. Second, potential interactions between TAOK1 and other pathways, such as the phosphoinositide 3-kinase/protein kinase B and mammalian target of rapamycin pathways, may be key to influencing atherosclerosis and have not been explored in this paper. Third, we did not test other key components of the NF-κB signaling pathway such as inhibitor of nuclear factor kappa-B alpha and IκB kinase. Finally, due to the incomplete understanding of TAOK1 mechanisms, its potential additional effects on atherosclerosis have not been further investigated. Future studies should explore these interactions to provide a more comprehensive understanding of the molecular mechanisms by which TAOK1 affects vascular pathologies.

Conclusions

In conclusion, our study reveals that TAOK1 exerts a protective influence on HUVECs under oxidative stress by modulating key cellular processes and signaling pathways. The interaction between TAOK1 and CDC20, along with the involvement of NF-κB and Wnt/β-catenin pathways, constitutes a key component of this protective role, offering fresh insights into the molecular underpinnings of endothelial cell dysfunction in vascular disease. These findings not only enhance our understanding of endothelial cell biology in the context of atherosclerosis but also point to potential therapeutic strategies targeting TAOK1 and CDC20.

Availability of Data and Materials

The datasets used and analyzed during the current study are available from the corresponding author upon reasonable request.

Author Contributions

YQ, HZ and YT designed the research study. HD and JW performed the research. HZ, HD, and JW provided help and advice on the ELISA, western blot, and flow cytometry experiments. YQ and YT analyzed the data. All authors were involved in the drafting and critical revision of the manuscript. All authors have read and approved the final manuscript. All authors have participated sufficiently in the work and agreed to be accountable for all aspects of the work.

Ethics Approval and Consent to Participate

Not applicable.

Acknowledgment

Not applicable.

Funding

This research received no external funding.

Conflict of Interest

The authors declare no conflict of interest.

References

[1] O'Donoghue ML, Giugliano RP, Wiviott SD, Atar D, Keech A, Kuder JF, *et al*. Long-Term Evolocumab in Patients With Established Atherosclerotic Cardiovascular Disease. Circulation. 2022; 146: 1109–1119.

[2] Qiao L, Ma J, Zhang Z, Sui W, Zhai C, Xu D, *et al*. Deficient Chaperone-Mediated Autophagy Promotes Inflammation and Atherosclerosis. Circulation Research. 2021; 129: 1141–1157.

[3] Sankrityayan H, Rao PD, Shelke V, Kulkarni YA, Mulay SR, Gaikwad AB. Endoplasmic Reticulum Stress and Renin-Angiotensin System Crosstalk in Endothelial Dysfunction. Current Molecular Pharmacology. 2023; 16: 139–146.

[4] Adachi Y, Ueda K, Nomura S, Ito K, Katoh M, Katagiri M, *et al*. Beiging of perivascular adipose tissue regulates its inflammation and vascular remodeling. Nature Communications. 2022; 13: 5117.

[5] Attiq A, Afzal S, Ahmad W, Kandeel M. Hegemony of inflammation in atherosclerosis and coronary artery disease. European Journal of Pharmacology. 2024; 966: 176338.

[6] Zhang Y, Li JJ, Xu R, Wang XP, Zhao XY, Fang Y, *et al*. Nogo-B mediates endothelial oxidative stress and inflammation to promote coronary atherosclerosis in pressure-overloaded mouse hearts. Redox Biology. 2023; 68: 102944.

[7] Zhao Y, Shao C, Zhou H, Yu L, Bao Y, Mao Q, *et al*. Salvianolic acid B inhibits atherosclerosis and TNF-α-induced inflammation by regulating NF-κB/NLRP3 signaling pathway. Phytomedicine. 2023; 119: 155002.

[8] Evans BR, Yerly A, van der Vorst EPC, Baumgartner I, Bernhard SM, Schindewolf M, *et al*. Inflammatory Mediators in Atherosclerotic Vascular Remodeling. Frontiers in Cardiovascular Medicine. 2022; 9: 868934.

[9] Li L, Du Z, Rong B, Zhao D, Wang A, Xu Y, *et al*. Foam cells promote atherosclerosis progression by releasing CXCL12. Bioscience Reports. 2020; 40: BSR20193267.

[10] Jiang Y, Shen Q. IRF2BP2 prevents ox-LDL-induced inflammation and EMT in endothelial cells via regulation of KLF2. Experimental and Therapeutic Medicine. 2021; 21: 481.

[11] Yang Z, Huang Y, Zhu L, Yang K, Liang K, Tan J, *et al*. SIRT6 promotes angiogenesis and hemorrhage of carotid plaque via regulating HIF-1α and reactive oxygen species. Cell Death & Disease. 2021; 12: 77.

[12] Duan H, Zhang Q, Liu J, Li R, Wang D, Peng W, *et al*. Suppression of apoptosis in vascular endothelial cell, the promising way for natural medicines to treat atherosclerosis. Pharmacological Research. 2021; 168: 105599.

[13] Lagoumtzi SM, Chondrogianni N. Senolytics and senomorphics: Natural and synthetic therapeutics in the treatment of aging and chronic diseases. Free Radical Biology & Medicine. 2021; 171: 169–190.

[14] Xia Y, Andersson E, Anand SK, Cansby E, Caputo M, Kumari S, *et al*. Silencing of STE20-type kinase TAOK1 confers protection against hepatocellular lipotoxicity through metabolic rewiring. Hepatology Communications. 2023; 7: e0037.

[15] Zhang Z, Tang Z, Ma X, Sun K, Fan L, Fang J, *et al*. TAOK1 negatively regulates IL-17-mediated signaling and inflammation. Cellular & Molecular Immunology. 2018; 15: 794–802.

[16] Lin YM, Wu CH, Chu PH, Ouyang P. Cell cycle expression of FLJ25439, a cytokinesis-associated protein, is mediated by D-box recognition and APC/C-Cdc20 regulated degradation. Biochemical and Biophysical Research Communications. 2022; 630: 151–157.

[17] Komaravolu RK, Waltmann MD, Konaniah E, Jaeschke A, Hui DY. ApoER2 (Apolipoprotein E Receptor-2) Deficiency Accelerates Smooth Muscle Cell Senescence via Cytokinesis Impairment and Promotes Fibrotic Neointima After Vascular Injury. Arteriosclerosis, Thrombosis, and Vascular Biology. 2019; 39: 2132–2144.

[18] Feng X, Du M, Li S, Zhang Y, Ding J, Wang J, *et al*. Hydroxysafflor yellow A regulates lymphangiogenesis and inflammation via the inhibition of PI3K on regulating AKT/mTOR and NF-κB pathway in macrophages to reduce atherosclerosis in ApoE-/- mice. Phytomedicine: International Journal of Phytotherapy and Phytopharmacology. 2023; 112: 154684.

[19] Qu L, Tian Y, Wang F, Li Z. NOVA1 promotes NSCLC proliferation and invasion by activating Wnt/β-catenin signaling. BMC Cancer. 2022; 22: 1091.

[20] Wang B, Tang X, Yao L, Wang Y, Chen Z, Li M, *et al*. Disruption of USP9X in macrophages promotes foam cell formation and atherosclerosis. The Journal of Clinical Investigation. 2022; 132: e154217.

[21] Wang Z, Zhang L, Li L, Zhou M. Loss of OTUD6B Stimulates Angiogenesis and Promotes Diabetic Atherosclerosis. Diabetes, Metabolic Syndrome and Obesity: Targets and Therapy. 2022; 15: 3027–3038.

[22] Li J, Liu Z, Wang L, Xu H, Wang Y. Thousand and one kinase 1 protects MCAO-induced cerebral ischemic stroke in rats by decreasing apoptosis and pro-inflammatory factors. Bioscience Reports. 2019; 39: BSR20190749.

[23] Zhang H, Ge S, Ni B, He K, Zhu P, Wu X, *et al*. Augmenting ATG14 alleviates atherosclerosis and inhibits inflammation via promotion of autophagosome-lysosome fusion in macrophages. Autophagy. 2021; 17: 4218–4230.

[24] Hashimoto K, Oda Y, Nakagawa K, Ikeda T, Ohtani K, Akagi M. LOX-1 deficient mice show resistance to zymosan-induced arthritis. European Journal of Histochemistry: EJH. 2018; 62: 2847.

[25] Karunakaran D, Nguyen MA, Geoffrion M, Vreeken D, Lister Z, Cheng HS, *et al*. *RIPK1* Expression Associates With Inflammation in Early Atherosclerosis in Humans and Can Be Therapeutically Silenced to Reduce NF-κB Activation and Atherogenesis in Mice. Circulation. 2021; 143: 163–177.

[26] Barzegar Behrooz A, Talaie Z, Jusheghani F, Łos MJ, Klonisch T, Ghavami S. Wnt and PI3K/Akt/mTOR Survival Pathways as Therapeutic Targets in Glioblastoma. International Journal of Molecular Sciences. 2022; 23: 1353.

[27] Gao Y, Guo C, Fu S, Cheng Y, Song C. Downregulation of CDC20 suppressed cell proliferation, induced apoptosis, triggered cell cycle arrest in osteosarcoma cells, and enhanced chemosensitivity to cisplatin. Neoplasma. 2021; 68: 382–390.